Journal of Materials Chemistry A

Accepted Manuscript

ROYAL SOCIETY OF CHEMISTRY

www.rsc.org/materialsA

22 Jan. 2016

Recent Advances in the Photovoltaic Applications of Coordination Polymers and Metal Organic Frameworks

Rajnish Kaur[1,2], Ki-Hyun Kim[3*], A. K. Paul[1], Akash Deep[1,2*]

[1]Central Scientific Instruments Organisation (CSIR-CSIO), Sector 30 C, Chandigarh, 160030, India; [2]Academy of Scientific and Innovative Research, CSIR-CSIO, Sector 30 C, Chandigarh, 160030, India; [3]Department of Civil & Environmental Engineering, Hanyang University, 222 Wangsimni-Ro, Seoul 04763, Republic of Korea

Abstract

Coordination polymers and metal organic frameworks (CPs/MOFs) have attracted a great deal of attention in a variety of scientific fields due to their unique and intriguing structural properties. Photovoltaic applications of these porous polymers belong to a relatively new area of research. Current status of research on this subject amply highlights the usefulness of CPs/MOFs in improving the properties of next-generation photovoltaic devices (e.g., dye-sensitized solar cells). This review article was written to cover the recent advancements that have been achieved in this rapidly expanding area of research. It also compares and contrasts the energy conversion efficiencies in photovoltaic applications using different MOFs and other systems.

Key words: CP/MOF, photovoltaic, porous polymer, solar cell

Correspondence: [1,2]Tel: +91 172 2657811, Email: dr.akashdeep@csio.res.in
[3]Tel: +82 2220 2325, Fax: +82 2 2220 1945, Email: kkim61@hanyang.ac.kr

Content:

1. Introduction
2. Semiconducting properties in MOFs
3. Optical response and charge transfer characteristics of MOFs
4. Light harvesting properties of MOFs
5. MOFs as a quasi-solid electrolyte in DSSCs
6. MOFs as counter/working electrodes in DSSCs
7. MOFs in Perovskite solar
8. Performance review of MOF-based DSSCs with respect to other important nanomaterials
9. Conclusions

1. Introduction

Solar powered energy production is an indispensable venture in the 21st century.[1,2] The natural photosynthetic process has long inspired researchers to develop inorganic materials that can be used for photochemical conversion of solar energy into chemical energy.[3,4] The advancement of knowledge in this process has also inspired the development of molecular dyes that can convert photons into high-energy redox equivalents.[5] After more than a decade of development, the photosensitization of wide-band gap nanocrystalline semiconductors with adsorbed dyes has become a realistic option for solar cell applications. The underlying principles of these molecular dyes have led to the realization of dye-sensitized solar cells (DSSCs). DSSCs are considered technically and economically viable alternatives to p–n junction photovoltaic devices.[6-8] One of the major research tasks in the development of solar cells has been the achievement of high efficiencies.[9-11] In the case of DSSCs, recent efforts have improved the energy conversion efficiency to around 13-14%.[12-15] In a recent report, the co-photosensitization with an alkoxysilyl-anchor dye ADEKA-1 and a carboxy-anchor organic dye LEG4 has been reported to achieve significantly enhanced electron injection process from the light-excited dyes to the TiO_2 electrodes.[15] This particular cell displayed a high conversion efficiency of over 14% under one sun illumination.

In conventional p–n junction systems, the semiconductor material assumes the tasks of both light absorption and charge carrier transport. However, these two functions are separated in DSSCs. A sensitizer is anchored to the surface of a wide band semiconductor to facilitate the absorption of light. After light has been absorbed, charge separation takes place at the interface via photo-induced electron injection from the dye into the conduction band of the solid. Carriers are transported into the conduction band of the semiconductor and the charge is collected.[16-18] The schematic of a typical DSSC is presented in Fig. 1. A sensitizer with a broad absorption

band, in conjunction with a thin oxide nanocrystallite film, is the configuration typically used in DSSCs to harvest a certain fraction of sunlight. Harvesting of light over a large spectral range (extending from the UV to the near IR regions) is required for efficient conversion of incident photons into an electric current.[19,20]

Metal-organic frameworks (MOFs) represent a class of porous coordination polymers (CPs) that consist of metal ions linked together by organic bridging ligands.[21-24] The typical assembly approach and structure of an MOF are shown in Fig. 2.[25] The MOF compounds are mainly synthesized through solvothermal, hydrothermal, or self-assembly processes.[26-28] The sum of the physical properties of the inorganic and organic components, combined with possible synergistic effects, lead to intriguing properties in these materials. MOFs exhibit very large surface areas and pore volumes, which also account for their low densities.[29] MOFs have been investigated for a diverse range of applications including gas storage,[30-32] catalysis,[33,34] photocatalysis,[35-37] photoluminescence-based sensors,[38-40] and drug delivery.[41-43] The combination of a wide range of metal ions and a variety of organic ligands enables the desired properties of MOFs to be conveniently tuned vis-à-vis a particular application.[44] Lately, investigation into MOFs for photovoltaic processes has become one of the most exciting research venues for the development of future DSSCs.[45,46] Additionally, most of the reported MOFs in the literature are non-conducting, but some studies have suggested that the use of special ligands or structural doping in MOFs could extend their potential to energy harvesting and energy storage applications.[47]

The number of articles and reports covering the applications of MOFs in photovoltaic (PV) technologies has increased over the last few years. The initial progress achieved in the subject of light harvesting by MOFs was reviewed by Wang et al. in 2012.[48] However, the above review article mostly focused on the photocatalytic properties of MOFs and their possible roles in light harvesting applications. In this present review, we aim to cover the latest developments made in

the PV/DSSC applications of MOFs. For the sake of clarity, the structural features of the different MOFs covered in this review are summarized in Table 1.

2. Semiconducting properties in MOFs

In general, the semiconductors act as insulators at low temperatures and as conductors at high temperatures. The conduction of electricity requires the presence of electrons in conduction band or holes in semiconductors. The semiconductors are however characterized by their low band gap (typically 0.7-4 eV)[49]. At low temperature, they may have a completely full valence band without facilitating the conduction; this is accounted by the forbidden energy level zone between the valence and conduction bands[49]. However, such forbidden zone is considerably small enough so that a great number of electrons can move across this gap upon the supply of sufficient energy (e.g. thermal excitation)[49]. Experimentally, the UV-Vis spectroscopic characterization is useful to depict the energy and nature (direct or indirect) of band gap, while information on the type of the semiconductor can be assessed by photoluminescence (PL) analysis. More rigorous studies, such as dielectric constant measurement, can be employed further to estimate the concentration of carrier contained in a given material.

As one of the pioneering works, Xamena et al.[50] articulated their theory on semiconducting properties of MOF-5. The authors experimentally explored the electrostatic potential and charge density of the material. The photovoltaic application of MOF-5 was demonstrated by plotting the current-voltage (I-V) curve and photocurrent spectrum (Fig. 3). Accordingly, it was suggested that the origin of the quantum dot like properties of MOF-5 was due to ZnO metal clusters. The presence of inorganic semiconductor quantum entities (such as dots or wires) in close contact with organic molecules enabled the tunable optical properties of this material. This study is considered to be one of the foundation stones that stimulated further exploration into the

photovoltaic potential of various MOFs. Alvaro et al.[51] made further assessments on the semiconducting behavior of MOF-5. They proposed the assembly of a photovoltaic solar cell consisting of a thin layer of MOF-5/DMF paste deposited onto a transparent indium tin oxide (ITO) electrode. Here, a platinum electrode was placed on top of the cell and the layer area and thickness were adjusted (using double-sided adhesive tape) to be 1×1 cm^2 and 50 μm, respectively. The performance of this solar cell was analyzed using a solar simulator (525 W, AM1.5 filter) in terms of the open-circuit voltage (V_{OC}), short-circuit current (I_{SC}), and fill factor (FF). These values were determined to be 0.33 V, 0.7 μA, and 44%, respectively.

Kobayashi et al.[52] demonstrated some unique properties like optical bandgap, p-type semiconductivity, and redox activity using a dithiolene based $Cu[Ni(pdt)_2]$ MOF (pdt^{2-} = pyrazine-2,3-dithiolate). The electronic conductivity was related with strong metal-ligand orbital interactions that took place within the molecular transition metal dithiolene complexes. The presence of diffuse reflectance spectra of $Cu[Ni(pdt)_2]$ in the UV-visible-near IR range implied an optical bandgap of approximately 2 eV. The conductivity measured initially as 10^{-8} S/cm (at room temperature) was improved substantially (e.g., by 4 orders of magnitude) through the doping of I_2 as an oxidant. The porosity of the MOF was nonetheless retained even after the doping. Another MOF, $Al_2(BDC)_3$ has also been suggested for its semiconducting properties.[53] The configuration of this system is shown in Fig. 4. The presence of an organic guest (1,4-dimethoxybenzene) was reported to strongly influence the efficiency of the device. The large porosity of this MOF allowed for the inclusion of photoactive guests within the intracrystalline space. Consequently, the resulting cell exhibited relatively efficient photovoltaic activity. Maintaining the film thickness at 2.7 μm, the authors observed that the values of the short circuit current density (J_{SC}) and open circuit potential (V_{OC}) were 36.2 μA/cm^2 and 361.339 mV, respectively. Lin et al.[54] reported the tunability of the band gaps in zinc-based MOFs via two

different approaches: (i) by changing the cluster size of the secondary building unit (SBU) or (ii) by alternating the conjugation of the organic linker. These approaches were effective in narrowing the material's band gap. It was also pointed out that the observed change in the band gaps could also be attributed to the combined effects of some other factors such as the cluster size, electronic effects (e.g., electron−phonon coupling and shape effects), vacancies, and surface defects. Recently, Usman et al.[55] proposed the self-assembly of a three-dimensional strontium-based metal–organic framework $[Sr(Hbtc)(H_2O)]_n$ via the reaction of $Sr(NO_3)_2$ with 1,2,4-benzenetricarboxylic acid. Semiconducting properties of this MOF were studied by both theoretical calculations and experimental measurements. Investigations on temperature-dependent DC conductivity, near-room-temperature AC conductivity, diffuse reflection spectra, and photoluminescence revealed the band gap as 2.3 eV, which was comparable to those of CdSe, CdTe, ZnTe, and GaP. Interestingly, the $[Sr(Hbtc)(H_2O)]_n$ MOFs may hence find potential applications in optoelectronic devices due to such unique properties.

In early studies, researchers primarily focused on the optical band gap properties of MOFs to assess their capacity as semiconductor (as in the case of MOF-5). However, more pieces of evidence should be gained to reach such a conclusion. Note that the MOF-5 has a large optical band gap, while maintaining low density of charge carriers in a highly localized manner. Hence, charge delocalization (and associated conductivity) in MOF-5 may not be realized or reproduced with desired efficiency. Likewise, MOFs are not the actual semiconductors, but they can still exhibit photocatalytic properties to serve as sensitizing dyes in DSSCs (like the plant chromoplasts). Although certain MOFs are reported to have some of unique semiconducting properties (e.g., quantum confinement studies, effect of n-/p- type doping, measurement of charge carrier concentration through dielectric properties), they need to be investigated further to elucidate their energy transfer mechanisms.[52,55]

3. Optical response and charge transfer characteristics of MOFs

It was reported that the optical response (or band gap modification), which is critical to PV applications, can be engineered through rational functionalization of the linking unit of titanium-based MOFs (e.g., MIL-125).[56] According to the density function theory (DFT), if a rational selection is made for the substituent of the aromatic linker, the optical response of MIL-125 can be tailored to allow for absorption in the visible region. Kent et al.[57] proposed photoactive Ru(II)-bpy (bpy = 2,2'-bipyridine) building blocks for the preparation of microscale MOFs (Fig. 5). These MOFs were characterized as having "antenna" like behavior with high electron transfer efficiencies (>98%). Efficient electron transfer was demonstrated through oxidative and reductive quenching of the photoluminescence of MOFs at the MOF/solution interface. This behavior was linked to the rapid energy migration that occurred over several hundred nanometers. As such, this work demonstrated that MOFs are a viable material for harvesting light for energy conversion through an excited state quenching and electron transfer processes.

A combination of a highly stable Zn-based MOFs (host framework) and methyl viologen (guest molecule) was proposed in an attempt to improve the electron transfer characteristics of CPs.[58] This supramolecular assembly allowed both the donor and acceptor molecular entities to be composed in a well-defined manner (Fig. 6). Manipulating structural arrays, adjusting donor–acceptor connections, and changing the distances of radical ion pairs were suggested as possible strategies to inhibit charge recombination. This system is considered to be the first MOF-based host–guest material that exhibits both photo- and thermal-induced electron transfer behavior.

Based on the simulation methods, the optical properties of Cd/Zn-based MOFs were examined to assess their synthesis conditions, stability, electronic structure, chemical bonding, and applicability in photovoltaic devices.[59] DFT calculations with different types of pseudo-potential

generalized gradient approximation-Perdew, Burke, and Ernzerhof (GGA-PBE) functions were implemented using the Vienna ab initio simulation package (VASP) code. The optical properties of Cd/Zn-based MOF-5 were calculated using the CASTEP module (a materials modelling code based on a first-principles quantum mechanical description of electrons and nuclei) of the Material Studio 5.0 program; accordingly, the semiconductor-type properties of these compounds (with a band gap of 3.6 eV) should be feasible for electronic applications.

4. Light harvesting properties of MOFs

Light harvesting capacity of MOFs is primarily dependent upon the linker characteristics. A majority of the linkers used in the development of MOFs for different applications are basically capable of absorbing light from UV to blue regions. However, there are reports for certain new candidates, e.g. 2,5-dihydroxyterephthalic acid (H_4DOBDC) and 2-amino terephthalic acid (NH_2-bdc) that have enhanced potential for harvesting of visible light spectrum[60,61]. The presence of conjugated π-electrons in these linkers can be correlated with the improved light absorption properties of the related MOFs. The transition of conjugated π-electrons from the chromophores to the metal centres can lead to effective generation of electron-hole pairs. The use of the organic linker H_4DOBDC has been explored in the synthesis of a p-type MOF (i.e., Ti(IV)-based NTU-9) with visible-light driven photoresponse[60] The resulting MOF displayed strong absorption in the visible region (absorption reaching up to 750 nm) with a bandgap of 1.72 eV. In some photoelectrochemical studies, the NTU-9 was found to have photoactivity under visible light illumination ($\lambda > 400$ nm). The use of NH_2-bdc linker has been reported to induce optically tunable properties in MIL-125 (TiO_2 based MOF)[61]. The band gap of this MOF could be modified through rational functionalization of the linking unit. A decrease in the band gap was observed with the use of monoaminated bdc-NH_2 due to the donation of N 2p electrons

206 to the aromatic linker. As such, a red-shifted band was formed above the valence-band edge of
207 MIL-125. The use of diaminated linker bdc-$(NH_2)_2$ and other functional groups (−OH, $-CH_3$,
208 and −Cl) could also facilitate the control of the optical response. The application of bdc-$(NH_2)_2$
209 linking unit was hence suggested to achieve a fairly low band gap (1.28 eV) in MIL-125. The
210 synthesise of Zr_6O_{32} units with the linker NH_2-bdc (or 2-aminoterephthalate) has also been
211 proposed for a visible light absorbing UiO-66-NH_2 MOF.[62] The UV-vis diffuse reflectance
212 studies were carried out to characterize the above MOF with an optical bandgap of 2.75 eV at
213 450 nm absorption band-edge

214 The selection of organic linker defines the light absorption characteristics of most of the
215 MOFs. In one of the report, the inorganic Fe_3-μ_3-oxo clusters have been suggested to play their
216 role in achieving visible light absorption of Fe(III)-MOF.[63] This MOFs could absorb photons
217 with energy comparable to the band gap of traditional semiconductor based photocatalysts, such
218 as TiO_2. An efficient photocatalytic performance of this MOF was proven via the degradation of
219 Rhodamine 6G in aqueous solutions.

220 The widening of light absorption profile of MOFs has also been suggested through formation
221 of their composites with materials such as quantum dots, graphene, CNTs and semiconductor
222 nanoparticles. A ZnO@ZIF-8 heterostructure has been proposed as a useful material due to its
223 photo-electrochemical response (Fig. 7).[64] To form this heterostructure, ZnO nanorods were used
224 as both the template and the source of Zn^{2+} ions to synthesize ZIF-8. The template method was
225 suggested as an effective strategy for fabricating MOF core−shell heterostructures because the
226 size and morphology of the desired product can be controlled in a straightforward manner. Upon
227 excitation with light (<380 nm), photo-generated carriers in the ZnO structure either recombined
228 with each other or migrated to surface trapping sites to react with redox species present on the

surface or in solution. The use of ZnO@ZIF-8 nanorod arrays improved the photocurrent response because the presence of ZIF-8 minimized recombination charge losses.

Jin et al.[65] reported the light harvesting properties of porphyrin-based MOFs. Enhanced light harvesting characteristics were reported by coupling MOFs with CdSe/ZnS (core/shell) quantum dots. This strategy is illustrated in Fig. 8. They suggested that the photon-generated excitons in the QDs were transferred to the MOFs in the form of resonance energy. Furthermore, observing the photoluminescence (PL) of MOFs, caused by energy transfer from QDs, confirmed the light harvesting of the QD−MOF hybrids. Light harvesting even occurred in the spectral regions where the MOFs have little absorptivity. As such, QD−MOF hybrids were reported to harvest photons well beyond the absorption spectrum of the MOF. Through time-resolved emission studies, these authors showed that this process utilized two steps. In the first step photoexcitation of the QDs took place, and in the second step energy transfer to the MOFs proceeded with efficiencies of more than 80%.

5. MOFs as a quasi-solid electrolyte in DSSCs

A magnesium-based MOF polymeric composite was proposed as a candidate for the enhancement of DSSC performance.[66] Fig. 9 describes the preparation of this polymer composite via a UV-induced free-radical process. This MOF was used as an electrolyte for quasi-solid DSSCs. The photovoltaic performance was strongly influenced by the amount of MOF present in the UV-cured polymer networks. In particular, this approach improved the V_{OC} of the DSSC (leading to a 4.8% increase in the solar energy conversion efficiency) and yielded outstanding long-term durability. In another report, the feasibility of metal-organic skeleton-based gel electrolytes was tested for high efficiency quasi-solid-state DSSCs.[67] The sponge-like porous matrix of a metal–organic gel (MOG) was synthesized by coordinating Al^{3+} and 1,3,5-

benzenetricarboxylate (H_3BTC). This material demonstrated an excellent ability to accommodate a variety of electrolyte ingredients. The MOG electrolyte was able to penetrate into the photoanode film and ensured good interfacial contact. At optimized conditions, the short circuit current density of gel-state cells improved to yield a high conversion efficiency of over 8.60%; this value was only a little lower than that of a liquid-state cell (9.13%).

6. MOFs as counter/working electrodes in DSSCs

MOFs have been reported for the production of improved electrode systems in DSSCs. In this regard, a highly efficient Pt-free DSSC was proposed by using a counter electrode of cobalt sulfide (CoS) nanoparticles synthesized via surfactant-assisted preparation of the MOF ZIF-67.[68] ZIF-67 consisted of cobalt cations as the metal source and 2-methylimidazole as the organic ligand, which were assembled to yield CoOx with a pore size of around 0.34 nm. This CoOx structure can be further converted into CoS through a simple sulfide conversion, as shown in Fig. 10. The use of this novel material as a counter electrode yielded a solar-to-electricity conversion efficiency of 8.1%.

In another recent report, ZIF-8 was also proposed as a material for the interfacial modification of DSSCs.[69] This modification utilized a post-treatment strategy to enhance the open-circuit voltage (V_{OC}). Briefly, TiO_2 photoanode interface was decorated by first sensitizing with the dyes. It was then followed by the overlayer growth of ZIF-8 with another round of dye-sensitization (TiO_2/dye/ZIF-8/dye surface) (Fig. 11). These authors reported the best conditions for optimum photovoltaic property of ZIF-8 such as the growth time of 7 min and post-treatment of the photoanode for 2 times. The energy barrier effect of ZIF-8 was accounted to the enhancement of Voc and electron lifetime. Although the absorption of dyes on ZIF-8 may hamper the electron injection, the very first layer step of anchoring dyes onto the TiO_2 was

ensured the efficiency of photocurrent output. In fact, the additional dyes adsorbed onto ZIF-8 further contributed to the enhancement of short-circuit photocurrent (Jsc).

There was also an attempt to use MOF-5 and MOF-177 films as the working electrodes in DSSCs. Feldblyum et al.[70] investigated the photo-electrochemical responses of these materials by growing films on carboxylic acid-terminated conductive fluorine-doped tin oxide substrates. As shown in Fig. 12, to construct this electrochemical cell, platinum wire and Ag/Ag^{+} were used as the counter electrode and quasi-reference electrode, respectively. Exposure of the MOF film to white light illumination in the presence of acetonitrile (as an electrolyte) elicited measurable photocurrents.

Typical V_{OC} values of TiO_2-based DSSCs are known to lie between 0.7 and 0.8 V.[71] However, these values deviate from the theoretical maximum V_{OC} value of 0.95 V.[71] Interestingly, an MOF-based working electrode has been proposed as a promising material for improving the open circuit voltage of dye-sensitized solar cells.[71] The performance of DSSCs was investigated using a TiO_2 electrode with coated layers of a zinc imidazolate framework (ZIF-8). The current-voltage (I–V) characteristics were studied to explain the increase in the Voc due to the inhibited interfacial charge recombination as a result of introduction of ZIF-8 shell material. The authors observed a linear relationship between the thickness of the ZIF-8 coating layer and the V_{OC} values. It was demonstrated that the V_{OC} values could be rationally controlled by adjusting the growth time of ZIF-8. After the growth of the ZIF-8 layer (40 min), the V_{OC} increased considerably from 741 mV to 796 mV, which was an increase of 55 mV compared to that of the electrode with only TiO_2 (Table 2). Since the TiO_2/ZIF-8 electrode inhibited the injection of electrons from dyes into the conduction band edge of TiO_2, the short circuit current was also decreased.

A copper-based MOF was developed via the layer-by-layer (LbL) synthesis technique.[72] The potential role of this platform as a light-absorbing layer in TiO_2-based solar cells was investigated. Iodine doping of MOFs was suggested as a method to improve the conductivity and charge-transfer reaction across the TiO_2/MOF/electrolyte interface. It was highlighted that appropriate assembly of MOFs into TiO_2 films can drastically influence the electron transportation behavior. Several layers of the MOF film were deposited via the LbL technique onto FTO glass that was covered with a TiO_2 film, as shown in Fig. 13. These authors also demonstrated that the structural features of the Cu-MOF remain intact, even after film formation. The photovoltaic performance was measured at various cycles of the LbL process. The HOMO−LUMO energy gap and the positions of the iodine-doped copper MOFs were suitable for use as a sensitizing layer in TiO_2-based liquid junction photovoltaic cells. Copper-based MOFs have also been explored to sensitize TiO_2-MWCNTs/FTO composite films.[73] The enhanced conductivity of the MOF, imparted via iodine doping, improved the conversion efficiency of the solar cell by nearly 60%. Fig. 14 depicts the current-voltage curves of the cells with FTO-glass/TiO_2/Cu-MOF/electrolyte/Pt, FTO-glass/TiO_2/Cu-MOF/electrolyte/Pt, and FTO-glass/TiO_2-MWCNTs/Cu-MOF/electrolyte/Pt configurations. The results of these studies consistently indicate that the desired characteristics can be improved by the rational selection of the MOF.

The in-situ conversion of MOFs into some other useful semiconducting nanostructures has also been proposed to exploit their application in photovoltaics. Li et al.[74] synthesized hierarchical ZnO (thicknesses of around 300–500 nm) from the decomposition of MOF-5 precursor and used them as a scattering layer in the bilayer photoanodes of DSSCs. The application of bilayer structure as optical scattering layer in photoanodes is important for enhancing the availability of incident photons. In this regard, the particles with submicrometer size in at least one dimension

are better alternatives than nanoparticles. Compared with the reference cell (FTO/ZnO), the ZnO parallelepipeds modified device (FTO/ZnO/MOF-5; calcined at 525 °C) was seen to have power conversion efficiency (PCE) of around 16.5%.

7. MOFs in Perovskite solar cells

Perovskite solar cells fall into a category of the fastest-advancing solar technologies. Their design incorporates a perovskite structured compound as the light-harvesting active layer. Hybrid organic-inorganic lead or tin halide-based materials have generally been used for such purpose. The use of mesoporous structured has enabled the development of solid-state perovskite with PCE exceeding 10%. MOFs with the same topology as inorganic perovskites can possess interesting properties such as coexistence of ferroelectric and magnetic ordering. These concepts have recently been conceptualized in the development of Perovskite solar cells. As one of the early examples in such respect, small crystal sized MOF-525 has been incorporated with perovskite to lead to a significant enhancement in the morphology and crystallinity of the perovskite thin film.[75] An application of 5 v/v% of MOF-525 suspension (20 mg/mL) in the MOF/perovskite precursor exhibited excellent cell characteristics, i.e. average PCE of 12.0%, open-circuit voltage (Voc) of 0.93 V, short-circuit current density (Jsc) of 23.04 mA/cm^2, and fill factor (FF) of 0.60. These results represent significant improvement relative to that of the control cell fabricated using only the pristine perovskite precursor solution (average PCE = 10.1%).

In another example of exploiting MOFs for perovskite solar cell, Vinogradov et al.[76] proposed the application of hydrothermally synthesized TiO_2–MIL-125 composite to produce a depleted perovskite/TiO_2–MOF heterojunction solar cell with the PCE of 6.4%. The selection of 3% MIL-125@TiO_2 yielded the values of Voc, Jsc, FF, and photocurrent response as 0.85 mV, 10.9 mA/cm^2, 0.69, and 39 μA/cm^2, respectively. Based on the density functional theory for first-

principles, Ghosh et al.[77] reported that the compressive strain can substantially increase the ferroelectric polarization effect of compounds like $C(NH_2)_3Cr(HCOO)_3$ and $(CH_3CH_2NH_3)Mn(HCOO)_3$. These researchers further suggested the possibility of tuning of ferroelectric polarization through appropriate thin film growth.

8. Performance review of MOF-based DSSCs with respect to other important nanomaterials

The fabrication of DSSCs has undergone numerous stages of improvements. Porphyrin-sensitized solar cells have shown excellent cell efficiencies, but the charge recombination between the acceptor species in the redox containing electrolyte and the injected electrons has generally been a shortcoming in these types of cells.[78] Because recombination reactions should be strongly dependent on the porphyrin molecular structure, researchers are required to find molecularly engineered porphyrin structures. New sensitizers or semiconductor systems, such as green grass, low molecular mass organogelator materials and ZnO rectangular prisms, have also been proven to be highly effective for achieving a broad photo-response in the available solar spectrum.[79-81] Semiconductor nanocrystals, including several metal chalcogenides (e.g., CdS, CdSe, PbS, and PbSe), molybdenum disulphide, graphene quantum dots, and carbon nanotubes, have been reported as viable building blocks for the design of next generation solar cells.[82-86]

The rate at which the separated charge carriers are driven toward opposing electrodes is a major factor governing the overall photocurrent generation efficiency of DSSCs. In this regard, porous nanocrystalline materials act as better photoanodes in photoelectrochemical cells because they help minimize charge recombination losses compared to other structures. In porous nanocrystalline materials, enhanced charge separation can be achieved through the semiconductor-electrolyte interface. CPs/MOFs are a category of highly porous nanocrystalline

materials that have been demonstrated to be highly efficient materials in various technological applications such as catalysis, gas storage and separation, chemo- and bio-sensing, etc. In addition, because of their unique optical properties, utilizing MOFs in photovoltaic applications has recently been investigated. As demonstrated by this review article, the role of MOFs for the development of DSSCs is important and has been explored in a variety of ways. The information summarized in Table 3 allows the performance of different MOFs to be compared with other important dye systems that are used in DSSCs. Because these types of MOF applications belong to a relatively new area of research, most of the currently available reports have focused on the exploitation of MOF materials for the construction of photoanodes. As shown in Table 3, utilizing MOFs in photoanodes appears to be highly beneficial in many respects. Most noticeably, the use of MOFs can effectively improve open circuit potential (V_{OC}) values, which should directly enhance the cell efficiency. The use of MOFs in the fabrication of counter electrode supports can expand the external surface areas and roughness factors relative to conventional Pt counter electrodes;[68] therefore, MOFs have great potential for the production of ecofriendly products (e.g., Pt-free DSSCs). With this system, a moderately high solar-to-electricity conversion efficiency of 8.1% could be achieved. The chemical and thermal stabilities of MOFs also represent an important advantage of MOF-based DSSCs compared to other types of sensitizing systems.

In most cases, the semiconducting, optical, charge separation, and light harvesting properties of MOFs have been exploited for the construction of novel electrodes. As reported by many recent studies, the synthesis of photoanodes has taken advantage of MOFs including ZIF-8, Cu-MOF (and its composites with CNTs), MIL-125, and $Al_2(BDC)_3$. MOFs are useful for achieving the desired values of the short circuit current/open circuit potential. Additionally, both MIL-125 and

ZIF-8 have been proven to offer enhanced V_{OC} values relative to other reported MOFs (e.g., $Al_2(BDC)_3$).

9. Conclusions

Some classes of CPs/MOFs have emerged as potent microporous semiconductor materials that are stable to light exposure. These materials are found to possess accelerated electron transfer rates compared to the general class of CPs/MOFs, which is an important feature for the realization of related photovoltaic capacities. Due to the diversity and tunability of CPs/MOFs, developing their core-shell structures should expand their applicability. Nanocomposite formation could also influence the crystallization process of CPs/MOF to enhance their semiconducting properties. The addition of catalytic components to the light-harvesting CPs/MOFs may also enable the realization of efficient artificial photosynthesis. Further improvements in the performance of CPs/MOF-based photovoltaic devices can be achieved by exploring different combinations of metal ions and ligands to tailor the electronic and light absorption properties. This is likely to be a significant research venue in the future.

Because relatively little research has been conducted on the photovoltaic applications of CPs/MOFs, only a limited number of research reports are currently available. Nonetheless, the underlying principles and the important roles of these polymers are likely to inspire future success in a variety of applications. The absorption of visible light by nanoporous CPs/MOFs is paving the way for the development of DSSCs with improved open circuit potentials and controlled charge recombination. To date, separate efforts have been made to design photoanodes and counter electrodes with CPs/MOFs, which have led to favorable cell efficiencies as high as 8.1%. If the different applicabilities of CPs/MOFs are merged for the construction of photoanodes and counter electrodes, it should be possible to obtain excellent

overall outputs in terms of the short circuit current, open circuit potential, fill factor, and cell efficiency. Moreover, if MOFs are conjugated with quantum dots, carbon nanotubes, nanoparticles, or porphyrin dyes, the utilization of MOFs with even broader light absorption characteristics should be possible. This could help lead to new methods to enhance transfer efficiencies. Some of the well-known assets of CPs/MOFs, including their solid-state device compatibility, thermal and chemical stability in nature, and stable optical properties, should be helpful for the development of a variety of photovoltaic applications. A very intriguing and emerging application of MOFs is also recognized in the field of Perovskite solar cells. Through an application of microporous nanocrystals of MOFs, it is possible to attain considerable enhancement in the morphology and crystallinity of perovskite thin films. The integration of three-dimensional perovskite structures with highly porous MOF coatings is expected to offer important advantages such as a high stability, large absorption coefficient, and high carrier mobility.

Acknowledgements

One of the authors (Rajnish Kaur) acknowledges the Department of Science and Technology (DST), India for her Research Fellowship. Financial support from the CSIR India project grant OMEGA/PSC0202/2.2.5 is also gratefully acknowledged. We are grateful to the Director, CSIR-CSIO, and Chandigarh, India. The third author also acknowledges partial support from the National Research Foundation of Korea (NRF) funded by the Ministry of Education, Science, and Technology (MEST) (No. 2009-0093848).

Authors' Biography

[1] Rajnish Kaur

Rajnish Kaur has completed her M.Sc in Physics and M. Tech in Nanotechnology. At present, she is a DST-INSPIRE senior research fellow at the AcSIR-CSIO, Chandigarh, India. Her research interests are in the photocatalysis and development of MOF-based hybrid dye sensitized solar cells. She has expertise in the synthesis of photoactive MOFs and quantum dots.

[2] Ki-Hyun Kim

Prof. Ki-Hyun Kim was at Florida State University for an M.S. (1984–1986) and at University of South Florida for a Ph.D. (1988–1992). He was a Research Associate at ORNL, USA (1992–1994). Then he moved to Korea and stayed at the Sangji University (1995–1998). In 1999, he joined Sejong University. In 2014, he moved to Dept. of Civil and Environmental Engineering at Hanyang University. His research areas focus on environmental analysis and air quality management. He was awarded a National Star Faculty in 2006. He is serving as an editorial member of journals (e.g. Air Pollution Research, Sensors, and Scientific World). He has published more than 370 articles in peer-reviewed international SCI journals.

[3] A. K. Paul

Dr. A. K. Paul has the M.Sc (Physics) from Punjabi University Patiala, M.Tech (Applied Optics) from IIT Delhi and Ph.D from Panjab University Chandigarh. He has served as Scientist/Professor for several years in CSIR-CSIO Chandigarh. He has a number of patents and international publications to his credit in the areas of applied physics, instrumentation, nanosensors, and biosensors.

[4]. Akash Deep

Dr. Akash Deep is working as a Scientist in the Nanotechnology lab of CSIR-CSIO, Chandigarh. He has M.Sc degree in organic chemistry and M.Phil in industrial chemistry. He completed his Ph.D (Chemistry) from IIT Roorkee in 2004 and has more than 11 years of professional research experience. Dr. Akash Deep has worked extensively in the fields of organometallic chemistry, solvent extraction, energy and environmental science, waste management and nanobiosensors. He has published more than 70 research papers in international journals.

References

1 K. Branker, K. M. J. M. Pathak and J. M. Pearce, *Renew. Sust. Energ. Rev.*, 2011, **15**, 4470.

2 G. R. Timilsina, L. Kurdgelashvili and P. A. Narbel, *Policy Research Working Paper*, 2011, **5845**, 1.

3 I. McConnell, G. Li and G.W. Brudvig, *Chem. Biol.*, 2010, **17**, 434.

4 T. F. Schulze and T. W. Schmidt, *Energy Environ. Sci.*, 2015, **8**, 103.

5 M. Grätzel, *Inorg. Chem.*, 2005, **44**, 6841.

6 A. C. Nwanya, F. I.Ezema and P. M. Ejikeme, *Int. J. Phys. Sci.*, 2011, **6**, 5190.

7 Q. Wang, S. Ito, M. Grätzel, F. Fabregat-Santiago, I. Mora-Seró, J. Bisquert, T. Bessho and H. Imai, *J. Phys. Chem. B.*, 2006, **110**, 25210.

8 T. Horiuchi, H. Miura, K. Sumioka and S. Uchida, *J. Am. Chem. Soc.*, 2004, **126**, 12218.

9 C. A. Bignozzi, R. Argazzi and C. J. Kleverlaan, *Chem. Soc. Rev.*, 2000, **29**, 87.

10 A. Kay and M. Grätzel, *Chem. Mater.*, 2002, **14**, 2930.

11 S. Ferrere, A. Zaban and B. A. Gregg, *J. Phys. Chem. B.*, 1997, **101**, 4490.

12 Q. Wang, S. Ito, M. Grätzel, F. Fabregat-Santiago, I. Mora-Seró, J. Bisquert, T. Bessho and H. Imai, *J. Phys. Chem. B.*, 2006, **110**, 25210.

13 A. Yella, H. W. Lee, H. N. Tsao, C. Yi, A. K. Chandiran, M. K. Nazeeruddin, E. W. G. Diau, C. Y. Yeh, S. M. Zakeeruddin and M. Grätzel, *Science*, 2011, **334**, 629.

14 S. Mathew, A. Yella, P. Gao, R. Humphry-Baker, B. F. E. Curchod, N. Ashari-Astani, I. Tavernelli, U. Rothlisberger, M. K. Nazeeruddin and M. Grätzel, *Nat. Chem.*, 2015, **6**, 242.

15 K. Kakiage, Y. Aoyama, T. Yano, K. Oya, J. Fujisawab and M. Hanaya, *Chem. Commun.*, 2015, **51**, 15894-15897

16 H. Yamaguchi, H. Hiramatsu, H. Hosono and T. Mizoguchi, *Appl. Phys. Lett.*, 2014, **104**, 153904.

17 M. Gratzel, *J. Photochem. Photobiol. A. Chem.*, 2004, **168**, 235.

18 S. Rühle, M. Shalom and A. Zaban, *ChemPhysChem*, 2010, **11**, 2290.

19 B. Tan and Y. Wu, *J. Phys. Chem. B.*, 2006, **110**, 15932.

20 Y.-L. Lee and Y.-S. Lo, *Adv. Funct. Mater.*, 2009, **19**, 604.

21 H.-C. Zhou, J. R. Long and O. M. Yaghi, *Chem. Rev.*, 2012, **112**, 673.

22 R. L. Martin and M. Haranczyk, *J. Chem. Theory Comput.*, 2013, **9**, 2816.

23 S. L. James, *Chem. Soc. Rev.*, 2003, **32**, 276.

24 J. L. C. Rowsell and O. M. Yaghi, *Micropor. Mesopor. Mat.*, 2004, **73**, 3.

25 J. Della Rocca and W. Lin, *Eur. J. Inorg. Chem.*, 2010, **2010**, 3725.

26 L. Wen, J. Zhao, K. Lv, Y. Wu, K. Deng, X. Leng and D. Li, *Crys.Growth Des.*, 2012, **12**, 1603.

27 Wen-bin Lin, *Eur. J. Inorg. Chem.*, 2010, **24**, 3725.

28 P. Horcajada, C. Serre, M. Vallet-Regí, M. Sebban, F. Taulelle and G. Férey, *Angew. Chem. Int. Ed.*, 2006, **45**, 5974.

29 S. T. Meek, J. A. Greathouse and M. D. Allendorf, *Adv. Mater.*, 2011, **23**, 249.

30 D. J. Collins and H.-C. Zhou, *J. Mater. Chem.*, 2007, **17**, 3154.

31 A. R. Millward and O. M. Yaghi, *J. Am. Chem. Soc.*, 2005, **127**, 17998.

32 S. Ma and H.-C. Zhou, *Chem. Commun.*, 2010, **46**, 44.

33 J. Lee, O. K. Farha, J. Roberts, K. A. Scheidt, S. T. Nguyen and J. T. Hupp, *Chem. Soc. Rev.*, 209, **38**, 1450.

34 P. Valvekens, F. Vermoortele and D. De Vos, *Catal. Sci. Technol.*, 2013, **3**, 1435.

35 P. Mahata, G. Madras and S. Natarajan, *J. Phys. Chem. B.*, 2006, **110**, 13759.

36 L.-L. Wen, F. Wang, J. Feng, K.-L. Lv, C.-G. Wang and D.-F. Li, *Cryst. Growth Des.*, 2009, **9**, 3581.

37 C. Wang, Z. Xie, K. E. deKrafft and W. Lin, *J. Am. Chem. Soc.*, 2011, **133**, 13445.

38 W. J. Rieter, K. M. L. Taylor and W. Lin, *J. Am. Chem. Soc.*, 2007, **129**, 9852.

39 Z. Hu, B. J. Deibert and J. Li, *Chem. Soc. Rev.*, 2014, **43**, 5815.

40 B. Chen, L. Wang, F. Zapata, G. Qian and E. B. Lobkovsky, *J. Am. Chem. Soc.*, 2008, **130**, 6718.

41 P. Horcajada, C. Serre, G. Maurin, N.A. Ramsahye, F. Balas, M. Vallet-Regí, M. Sebban, F. Taulelle and G. Férey, *J. Am. Chem. Soc.*, 2008, **130**, 6774.

42 C.-Y. Sun, C. Qin, X.-L. Wang and Z.-M. Su, *Expert Opin. Drug Deliv.,* 2012, **10**, 89.

43 J. D. Rocca, D. Liu and W. Lin, *Acc. Chem. Res.*, 2011, **44**, 957.

44 P. Horcajada, C. Serre, M. Vallet-Regí, M. Sebban, F. Taulelle and G. Férey, *Angew. Chem. Int. Ed.*, 2006, **45**, 5974.

45 S. Zhang, L. Han, L. Li, J. Cheng, D. Yuan and J. Luo, *Cryst. Growth Des.*, 2013, **13**, 5466.

46 M. Jahan, Q. Bao and K. P. Loh, *J. Am. Chem. Soc.*, 2012, **134**, 6707.

47 C. H. Hendon, D. Tiana and A. Walsh, *Phys. Chem. Chem. Phys.*, 2012, **14**, 13120.

48 C. Wang, Z. Xie, K.E. deKrafft and W. Lin, *ACS Appl. Mater. Interfaces*, 2012, **4**, 2288.

49 G. Horowitz, *J. Appl. Phys.* 2015, **118**, 115502 (2015).

50 F. X. L.i. Xamena, A. Corma and H. Garcia, *J. Phys. Chem. C.*, 2007, **111**, 80.

51 M. Alvaro, E. Carbonell, B. Ferrer, F. X. Llabrés i Xamena and H. Garcia, *Chem. Eur. J.*, 2007, **13**, 5106.

52 Y. Kobayashi, B. Jacobs, M.D. Allendorf and J.R. Long, *Chem. Mater.*, 2010, **22(14)**, 4120–4122.

53 H. A. Lopez, A. Dhakshinamoorthy, B. Ferrer, P. Atienzar, M. Alvaro and H. Garcia, *J. Phys. Chem. C*, 2011, **115**, 22200.

54 C.-K Lin, D. Zhao, W.-Y. Gao, Z. Yang, Y. Jingyun, X. Tao, G. Qingfeng, M. Shengqian and L. Di-Jia, *Inorg, Chem.*, 2012, **51**, 9039.

55 M. Usman, S. Mendiratta, S. Batjargal, G. Haider, M. Hayashi, N.R. Gade, J.-W. Chen, Y.-F. Chen and K.-L. Lu, *ACS Appl. Mater. Interfaces*, 2015, **7(41)**, 22767–22774.

56 C. H. Hendon, D. Tiana, M. Fontecave, C Sanchez, L. D'arras, C. Sassoye, L. Rozes, C. Mellot-Draznieks and A. Walsh, *J. Am. Chem. Soc*, 2013, **135**, 10942.

57 C. A. Kent, D. Liu, L. Ma, J. M. Papanikolas, T. J. Meyer, W. Lin, *J. Am. Chem. Soc*, 2011, **133**, 12940.

58 Y. Zeng, Z. Fu, H. Chen, C. Liu, S. Liao and J. Dai, *Chem. Commun.*, 2012, **48**, 8114.

59 L.-M. Yang, L. Ravindran, P. Vajeeston, S. Svelle and M. Tilset, *Micropor. Mesopor. Mat.*, 2013, **175**, 50.

60 J. Gao, J. Miao, P.-Z. Li, W.Y. Teng, L. Yang, Y. Zhao, B. Liu and Q. Zhang, *Chem. Commun.*, 2014, **50**, 3786-3788.

61 C. H. Hendon, D. Tiana, M. Fontecave, C. Sanchez, L. D'arras, C. Sassoye, L. Rozes, C. Mellot-Draznieks, A. Walsh, *J. Am. Chem. Soc.*, 2013, **135(30)**, 10942–10945.

62 J. Long, S. Wang, Z. Ding, S. Wang, Y. Zhou, L. Huang and X. Wanga, *Chem. Commun.*, 2012, **48**, 11656-11658.

63 K. G. M. Laurier, F. Vermoortele, R. Ameloot, D. E. De Vos, J. Hofkens and M. B. J. Roeffaers, *J. Am. Chem. Soc*, 2013, **135**, 14488-14491.

64 W.-W. Zhan, Q. Kuang, J.-Z. Zhou, X. J. Kong, Z.-X. Xie and L.-S. Zheng, *J. Am. Chem. Soc*, 2013, **135**, 1926.

65 S. Jin, H.-J. Son, O. K. Farha, G. P. Wiederrecht and J. T. Hupp, *J. Am. Chem. Soc*, 2013, **135**, 955.

66 F. Bella, R. Bongiovanni, R. S. Kumar, M. A. Kulandainathan and A. M. Stephan, *J. Mater. Chem. A.*, 2013, **1**, 9033.

67 J. Fan, L. Li, H.-S. Rao, Q.-L. Yang, J. Zhang, H.-Y. Chen, L. Chen, D.-B. Kuang and C.-Y. Su, *J. Mater. Chem. A.*, 2014, **2**, 15406.

68 S.-H. Hsu, C.-T. Li, H.-T. Chien, R. R. Salunkhe, N. Suzuki, Y. Yamauchi, K.-C. Ho and K. C.-W. Wu, *Sci. Rep.*, 2014, **4**, 6983.

69 Y. Li, C. Chen, X. Sun, J. Dou and M. Wei, *ChemSusChem*, 2014, **7**, 2469.

70 J. I. Feldblyum, E. A. Keenan, A. J. Matzger and S. Maldonado, *J. Phys. Chem. C.*, 2012, **116**, 3112.

71 Y. Li, A. Pang, C. Wang and M. Wei, *J. Mater. Chem.*, 2011, **21**, 17259- 17264.

72 D. Y. Lee, D. V. Shinde, S. J. Yoon, K. N. Cho, W. Lee, N. K. Shrestha and S.-H. Han, *J. Phys. Chem. C.*, 2014, **118**, 16328.

73 D. Y. Lee, C. Y. Shin, S. J. Yoon, H. Y. Lee, W. Lee, N. K. Shrestha, J. K. Lee and S. H. Han, *Sci. Rep.*, 2014, **4**, 3930.

74 Y. Li, Z. Che, X. Sun, J. Dou and M. Wei, *Chem. Commun.*, 2014, **50**, 9769-9772.

75 T.-H. Chang, C.-W. Kung, H.-W. Chen, T.-Y. Huang, S.-Y. Kao, H.-C Lu, M.-H. Lee, K. M. Boopathi, C.-W. Chu, K.-C. Ho, *Adv. Mater.*, 2015, **27(44)**, 7229–7235.

76 A. V. Vinogradov, H. Zaake-Hertling, E. Hey-Hawkins, A. V. Agafonov, G. A. Seisenbaeva, V. G. Kessler and V. V. Vinogradov, *Chem. Commun.*, 2014, **50**, 10210-10213.

77 S. Ghosh, D. D. Sante and A. Stroppa, *J. Phys. Chem. Lett.*, 2015, **6(22)**, 4553–4559

78 M. J. Griffith, K. Sunahara, P. Wagner, K. Wagner, G. G. Wallace, D. L. Officer, A. Furube, R. Katoh, S. Mori and A. J. Mozer, *Chem. Commun.*, 2012, **48**, 4145.

79 V. Shanmugam, S. Manoharan, A. Sharafali, S. Anandan and R. Murugan, *Spectrochim. Acta Mol. Biomol. Spectrosc.*, 2015, **135**, 947.

80 F. A. Al-Agel, M. Shaheer Akhtar, H. Alshammari, A. Alshammari and S. A. Khan, *Mater. Lett.*, 2015, **147**, 119.

81 L. Tao, Z. Huo, Y. Ding, Y. Li, S. Dai, L. Wang, J. Zhu, X. Pan, B. Zhang, J. Yao, M. K. Nazeeruddin and M. Gr¨atzel, *J. Mater. Chem. A.*, 2015, **3**, 2344.

82 M. Eskandari, V. Ahmadi, S. Kohnehpoushi and M. Y. rad, *Phys. E.*, 2015, **66**, 275.

83 Z. Wang, Q. Tang, B. He, X. Chen, H. Chen and L. Yu, *J. Power Sources*, 2015, **275**, 175.

84 H.-S. Kim, S. H. Im and N.-G. Park, *J. Mater. Chem. C.*, 2014, **118**, 5615.

85 J.-W. Lee, D.-Y. Son, T. K. Ahn, H.-W. Shin, I. Y. Kim, S.-J. Hwang, M. J. Ko, S. Su, H. Han and N.-G. Park, *Sci. Rep.*, 2014, **3**, 1050.

86 M.-L. Tsai, S.-H. Su, J.-K. Chang, D.-S. Tsai, C.-H. Chen, C.-I Wu, L.-J. Li, L.-J. Chen and J.-H. He, *ACS Nano*, 2014, **8**, 8317.

87 X. Fang, M. Li , K. Guo, J. Li, M. Pan, L. Bai, M. Luoshan and X. Zhao, *Electrochim. Acta*, 2014, **137**, 634.

88 Q. Tang, H. Cai, S. Yuan and X. Wang, *J. Mater. Chem. A*, 2013, **1**, 317.

89 A. Ramar, T. Soundappan, S.-M. Chenl, M. Rajkumar and S. Ramiah, *Int. J. Electrochem. Sci.*, 2012, **7**, 11734.

90 J. Velten, A. J. Mozer, D. Li, D. Officer, G. Wallace, R. Baughman and A. Zakhidov, *Nanotechnology*, 2012, **23**, 085201.

Table 1. Structural details of different MOFs reported for photovoltaic applications

MOF Acronym	**Metal Unit**	**Organic Ligand**	**Crystal Structure**	**Reference**
IRMOF-16	Zinc	terphenyl-4,4'-dicarboxylate (TPDC)	Cubic	47
MOF-5	Zinc	1,4-benzenedicarboxylic (bdc) acid	Cubic	47
MIL-125	Titanium	terephthalic acid	Octahedral	50
Ru(II)-bpy	Ruthenium	bpy = 2,2'-bipyridine		51
ZIF-8	Zinc	2-methylimidazole	Sodalite (SOD) zeolite	53
$Al_2(BDC)_3$	Aluminium	p-benzenedicarboxylate	Octahedral	54
MOF-177	Zinc	Benzenetribenzoic acid	Hexagonal	56
Cd-MOF-5	Cadmium	benzene-1,4-dicarboxylate (BDC).	Cubic	65
Fe(III)-based MOFs	Iron	1,3,5-benzenetricarboxylate	Rhomb-shaped	67
Cu-MOF	Copper	1,3,5-benzenetricarboxylate	Square planar	70

Table 2. Photovoltaic performance (in terms of the short circuit current density J_{SC}, open circuit potential V_{OC}, fill factor FF, and cell efficiency η) of TiO_2 and TiO_2/ZIF-8 electrode-based DSSCs with respect to different growth times, i.e., 5, 10, 15, 20, 25, 30, and 40 min[71]

Electrode	J_{sc}	V_{oc}	FF	η (%)
P25	9.79	741	0.70	5.11
P25/ZIF-8-5	9.67	756	0.71	5.21
P25/ZIF-8-10	10.28	753	0.69	5.34
P25/ZIF-8-15	9.85	766	0.69	5.19
P25/ZIF-8-20	8.96	777	0.69	4.80
P25/ZIF-8-25	8.36	783	0.69	4.49
P25/ZIF-8-30	8.19	786	0.71	4.57
P25/ZIF-8-40	7.90	796	0.68	4.31

Table 3. Comparison of DSSC performance of nanomaterials and CPs/MOFs

Major Configuration	Parameters				Remarks	Ref.
	J_{SC} (mA/cm^2)	V_{OC} (mV)	FF	η (%)		
Green grasses	2.199	593.55	0.3554	0.46	Photoanode	79
ZnO rectangular prism	8.91	725	0.51	3.3	Photoanode	80
Low molecular mass organogelator	17.36	741	0.75	9.61	Quasi-solid-state electrolyte	81
ZnO nanorod-based quantum dot	1.15	690	33	1.15	Photoanode	82
Titanium dioxide/calcium fluoride nanocrystallite	14.5	710	74.2	7.66	Photoanode	83
Organolead halide perovskite	17	900		9.7	Photoanode	84
Quantum dots	29.98	398	46.80	5.58	Photoanode	85
MoS_2	22.36	410	57.26	5.23	Photoanode	86
Graphene quantum dots	14.07	660	0.59	6.10	Photoanode	87
Double-layered polyaniline	13.4	728	0.67	6.58	Counter electrode	88
Carbon nanotubes-ZnO	12.06	450	49.81	2.15	Photoanode	89
Carbon nanotube/graphene nanocomposite	16.05	750	0.62	7.55	Counter electrode	90
π-bridge-acceptor zinc porphyrin dye	9.3	940	0.74	12.7	Photoanode of TiO_2-loaded dye	13
Molecularly engineered porphyrin dye, coded SM315	18.1	910	0.78	13	Photoanode	14
MOF-derived cobalt sulfide nanoparticles	14.7	784	0.71	8.1	Counter electrode	68
FTO/TiO_2/Cu-MOFs	1.22	430	00.51	0.27	Photoanode	72
FTO/TiO_2/MWCNT/Cu-MOFs	1.95	480	0.51	0.46	Photoanode	73
DMB@ $Al_2(BDC)_3$	36.20	361	40.46		Photoanode	53
ZIF-8/TiO_2	9.67	756	0.71	5.21	Photoanode	71
Hierarchical ZnO parallelepipeds prepared from a MOF precursor	8.13	663	0.68	3.67	Effective scattering layer in the	74

					bilayer photoanodes	
Zr-based porphyrin metal–organic framework (MOF-525)	23.04	930	0.60	12	Perovskite thin film hetero-junction	75
Perovskite/TiO_2/MIL-125 based heterojunction solar cells	10.9	850	0.69	6.4	Perovskite thin film hetero-junction	76

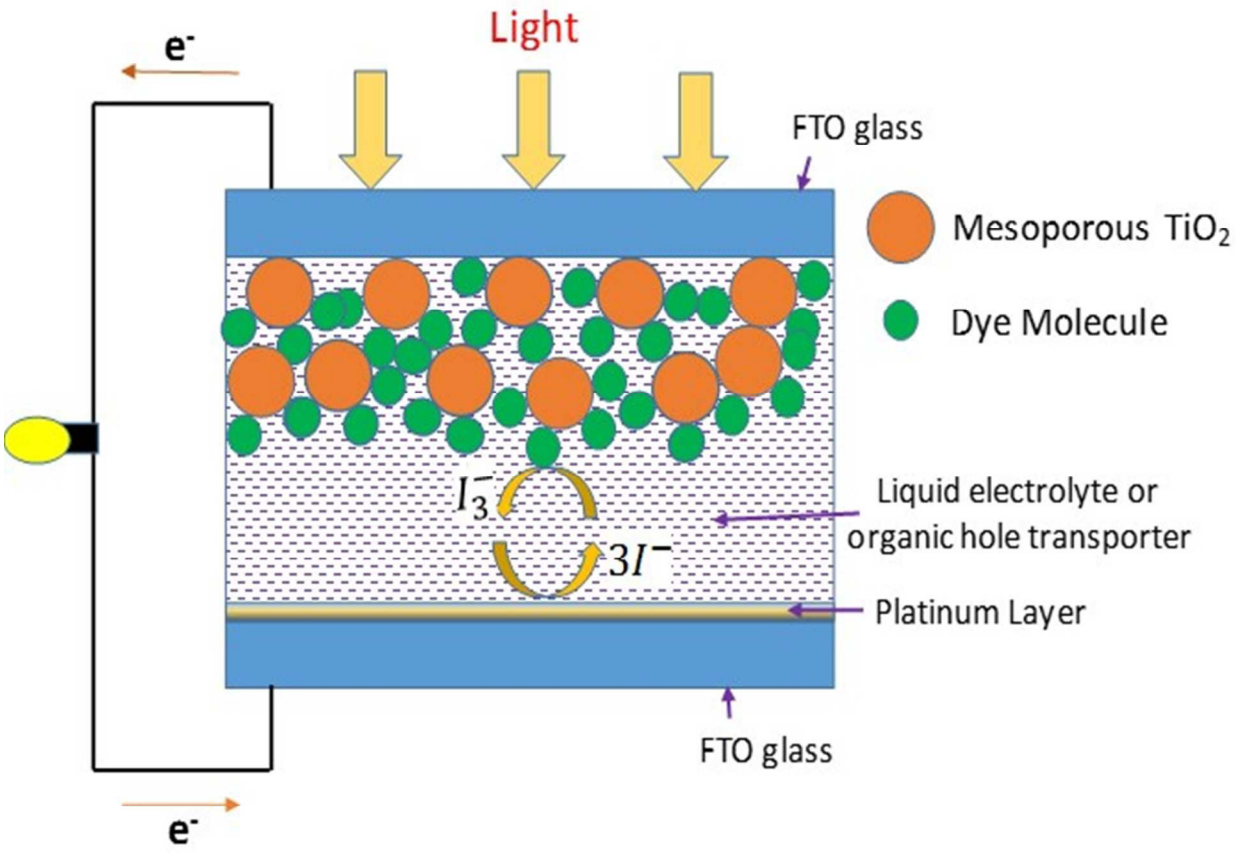

Fig. 1. Schematic diagram of a typical DSSC mechanism.

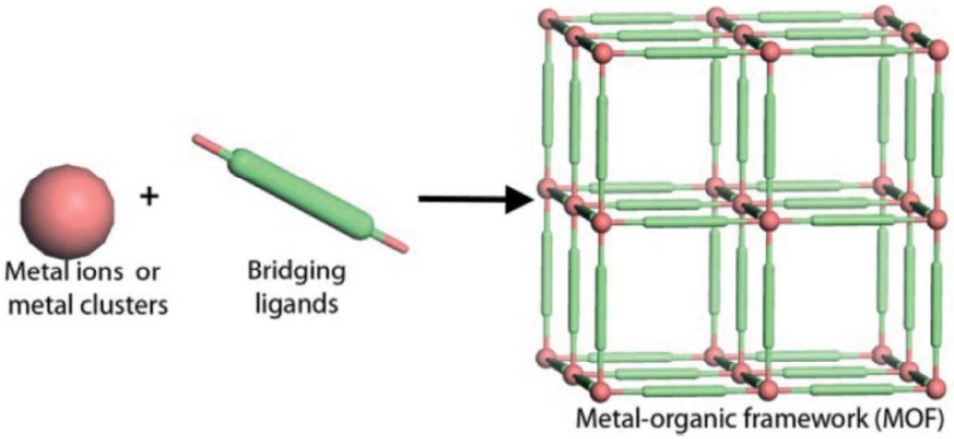

Fig. 2. A model for the structural assembly of an MOF.[25] Reprinted with permission from ref. 25. Copyright © 2010 John Wiley & Sons, Ltd.

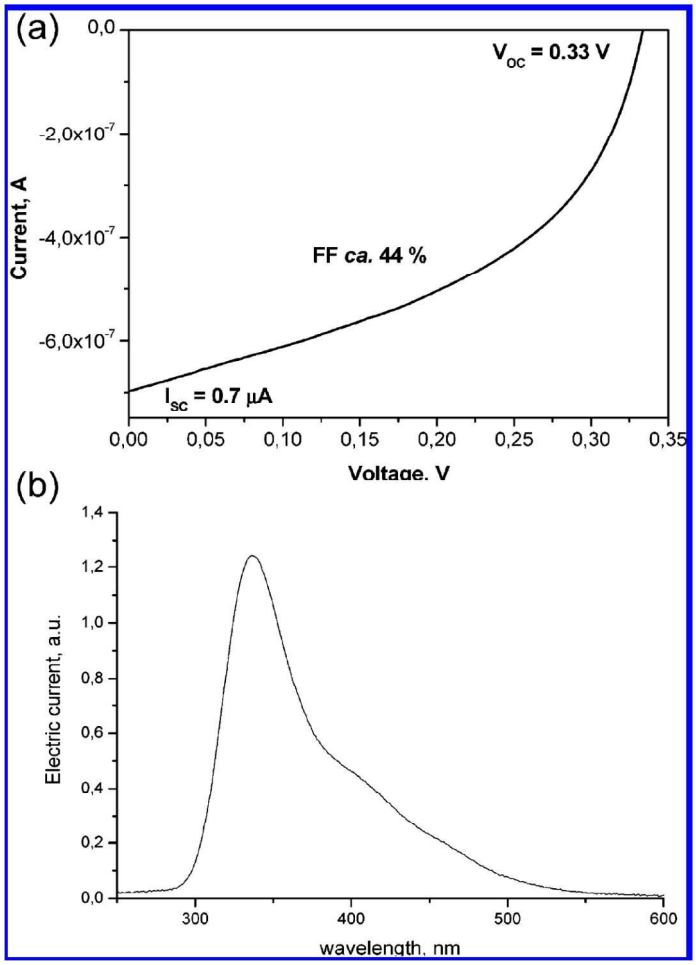

Fig. 3. (a) I-V curve obtained for the photovoltaic solar cell prepared with MOF-5 upon irradiation with an AM1.5-filtered lamp (525 W) using an ITO-glass electrode and (b) photocurrent spectrum of MOF-5 obtained with a transparent electrode consisting of ITO on glass.[50] Reprinted with permission from ref. 50. Copyright © 2007 American Chemical Society.

i

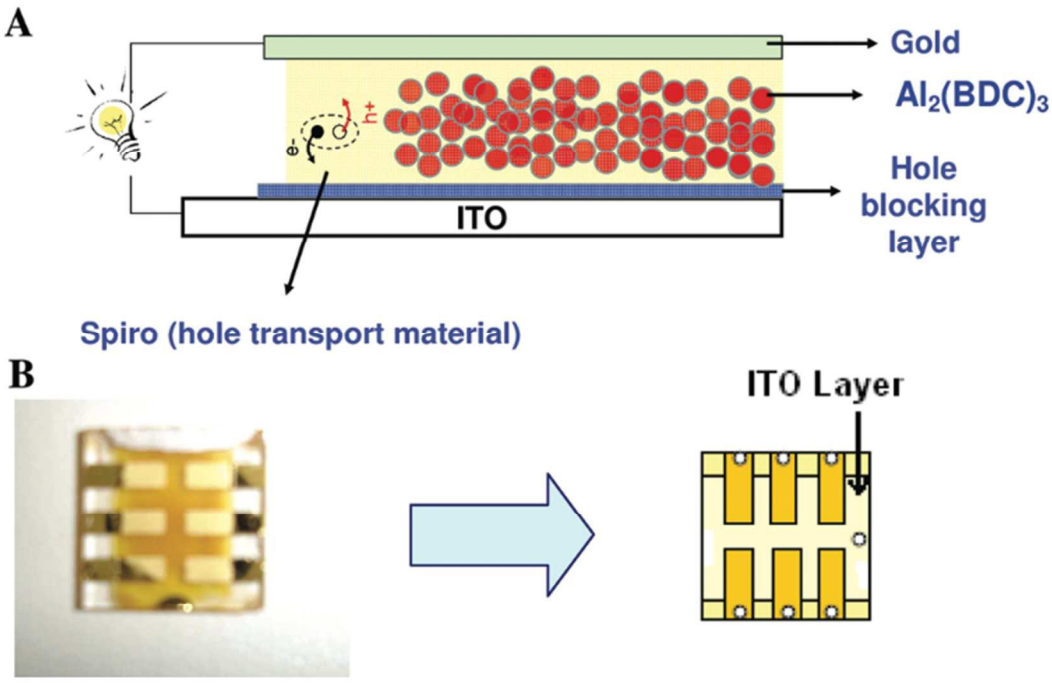

Fig. 4. (a) Configuration of the Al-MOF-based DSSC showing the compositions of the different layers and (b) photograph and scheme of the devices consisting of a series of six individual photovoltaic cells.[53] Reprinted with permission from ref. 53. Copyright © 2011 American Chemical Society.

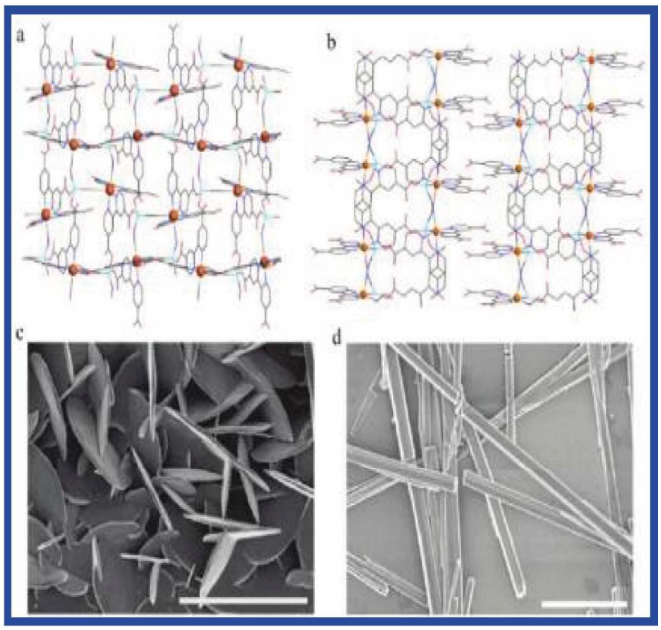

Fig. 5. SEM images of Ru(II)-bpy building blocks-based microscale MOFs.[57]
Reprinted with permission from ref. 57. Copyright © 2011 American Chemical Society.

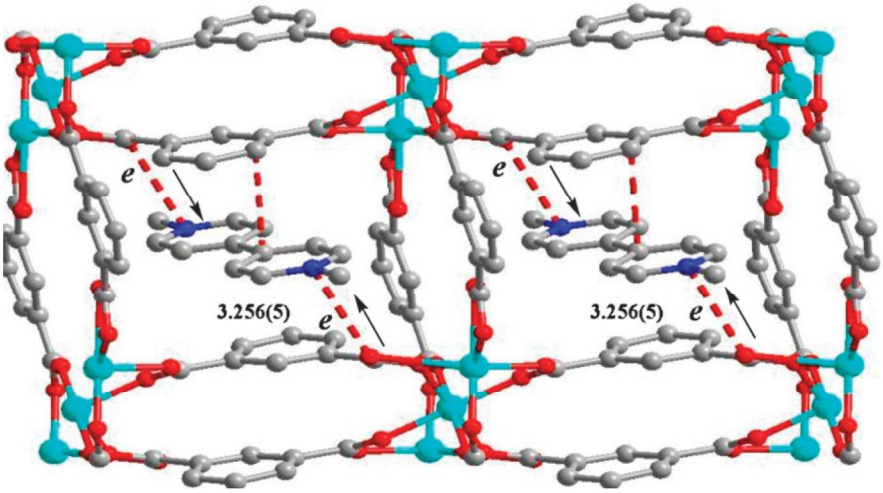

Fig. 6. A structural diagram of the MOF-based host–guest system.[58] Reprinted with permission from ref. 58. Copyright © 2012 Royal Society of Chemistry.

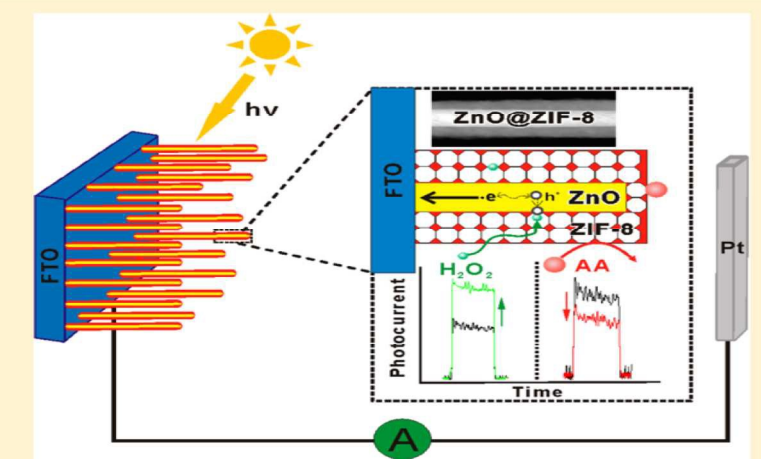

Fig. 7. Schematic illustration of ZnO@ZIF-8 nanorods.[64] Reprinted with permission from ref. 64. Copyright © 2013 American Chemical Society.

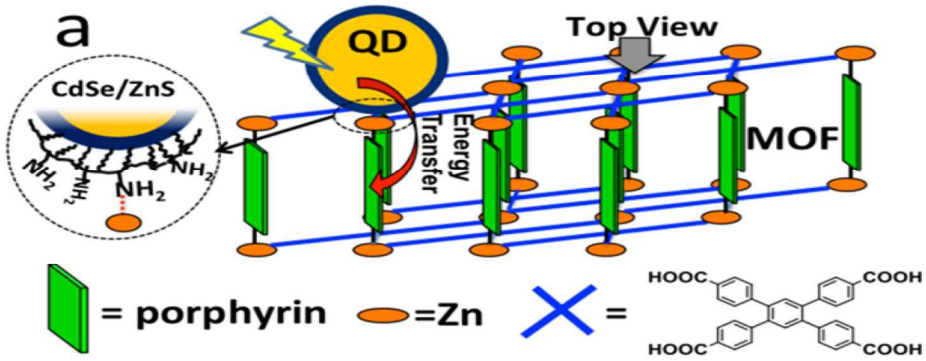

Fig. 8. Strategy for coupling the QD−MOF complex to improve the light harvesting characteristics.[65] Reprinted with permission from ref. 65. Copyright © 2013 American Chemical Society.

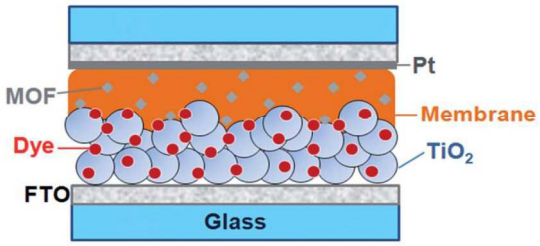

Fig. 9. DSSC assembly with Mg-MOF-based polymer electrolyte membrane.[66] Reprinted with permission from ref. 66. Copyright © 2013 Royal Society of Chemistry.

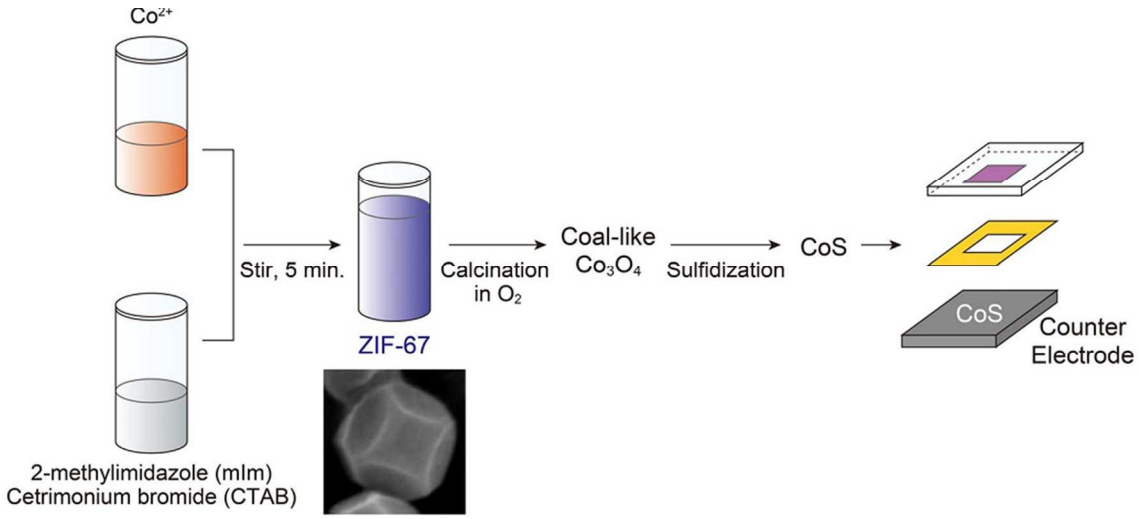

Fig. 10. Schematic of the fabrication procedure of cobalt sulfide as a Pt-replaced counter electrode for dye-sensitized solar cells.[68] Reprinted with permission from ref. 68. Copyright © 2014 Nature Publishing Group.

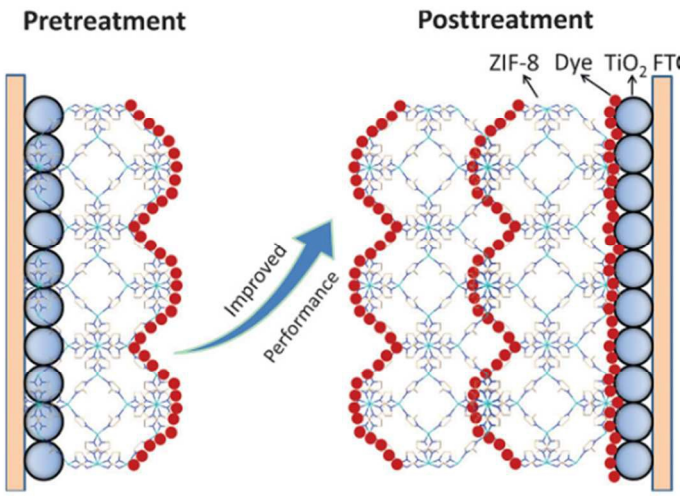

Fig. 11. Interfacial treatment of a DSSC by ZIf-8. Photoanode status is shown after sensitization in the pretreatment and post-treatment approaches.[69] Reprinted with permission from ref. 69. Copyright © 2014 John Wiley & Sons, Ltd.

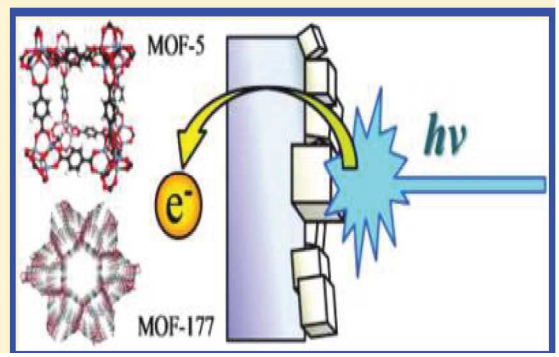

Fig. 12. Application of MOF-based thin films (MOF-5 and MOF-177) as the working electrode in DSSCs.[70] Reprinted with permission from ref. 70. Copyright © 2012 American Chemical Society.

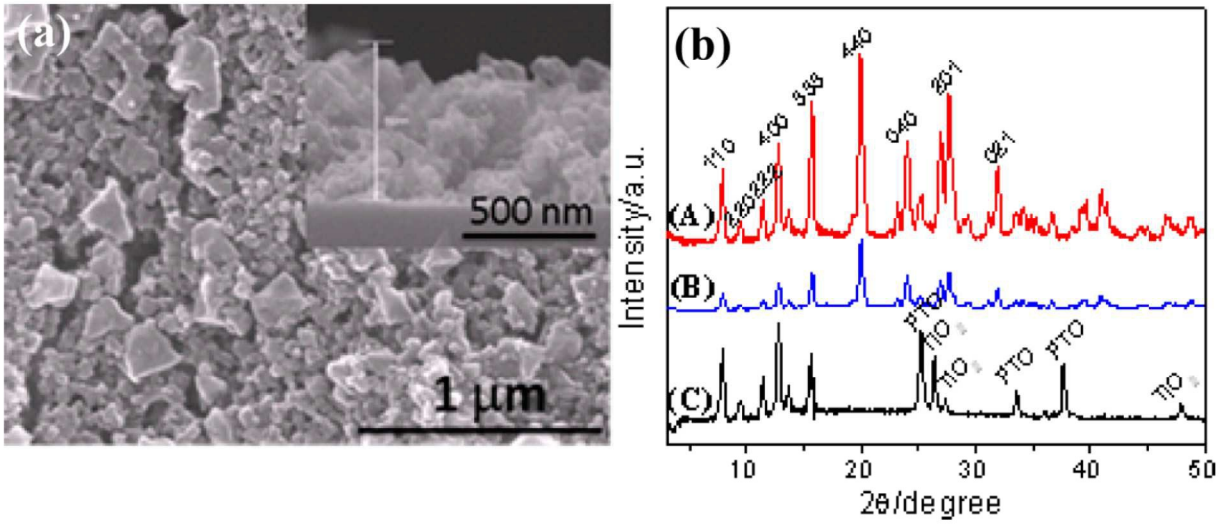

Fig. 13. (a) SEM view of Cu-MOF layers (10 cycles) on a glass substrate. (b) XRD patterns of (A) bulk powder Cu-MOFs, (B) powder collected from the film of Cu-MOFs on a glass substrate, and (C) film of Cu-MOFs and doctor-bladed TiO_2 film on an FTO-coated glass substrate.[72] Reprinted with permission from ref. 72. Copyright © 2014 American Chemical Society.

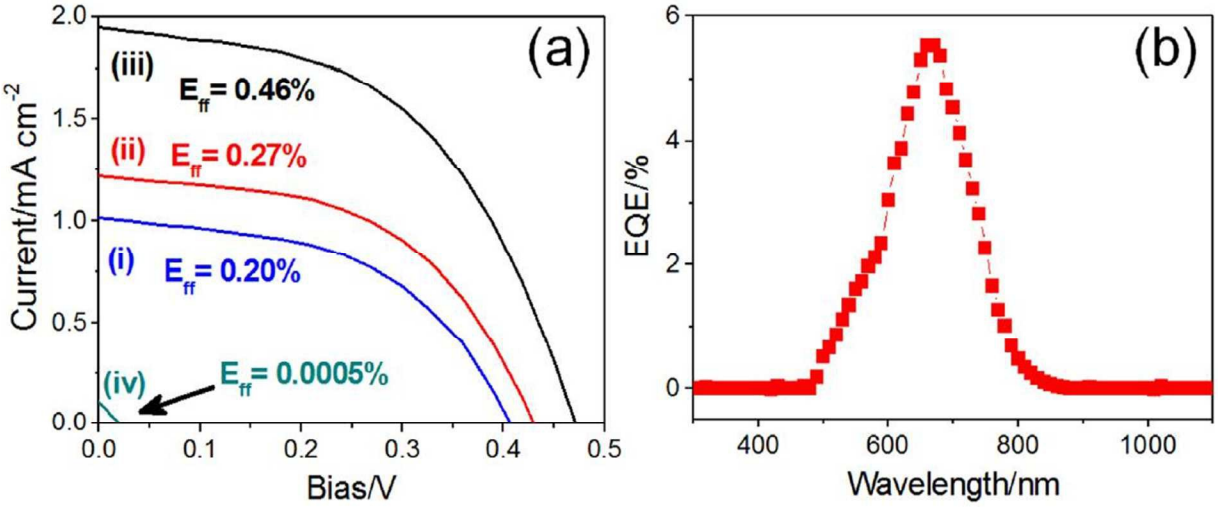

Fig 14. (a) Current-voltage curves of DSSCs with (i) FTO-glass/TiO_2, (ii) Cu-MOF/electrolyte/Pt, (iii) FTO-glass/TiO_2/Cu-MOF/electrolyte/Pt, and (iv) FTO-glass/TiO_2-MWCNTs/Cu-MOF/electrolyte/Pt configurations. (b) IPCE (incident photon-to-current efficiency) spectrum of the FTO-glass/TiO_2-MWCNTs/Cu-MOF/electrolyte/Pt configuration.[73] Reprinted with permission from ref. 73. Copyright © 2014 Nature Publishing Group.